



A novel hydrogel containing thioether group as selective support material for preparation of gold nanoparticles: Synthesis and catalytic applications

Pinar Ilgin^a, Ozgur Ozay^{b,c,*}, Hava Ozay^c

^a Department of Chemistry and Chemical Processing Technologies, Lapseki Vocational School, Canakkale Onsekiz Mart University, Canakkale, Lapseki, Turkey

^b Department of Bioengineering, Faculty of Engineering, Canakkale Onsekiz Mart University, Canakkale, Turkey

^c Laboratory of Inorganic Materials, Department of Chemistry, Faculty of Science and Arts, Canakkale Onsekiz Mart University, Canakkale, Turkey

ARTICLE INFO

Keywords:

Gold nanoparticle
Catalyst
4-Nitrophenol
Hydrogel

ABSTRACT

In this study, firstly N-metacrylamido thiomorpholine containing thioether group was synthesized as monomer. Then, p(AAm-co-MTM) hydrogels were prepared from the redox polymerization of acrylamide and N-metacrylamido thiomorpholine as a selective support material. p(AAm-co-MTM) hydrogel-gold nanoparticles were obtained as a result of the reduction of the selectively absorbed gold(III) ions by the hydrogel network using NaBH₄ as reducing agent. All materials were characterized using techniques such as SEM, EDX, TEM and XRD analysis. It was determined that p(AAm-co-MTM)-Au composite material has high catalytic activity for the reduction of 4-nitrophenol. The activation parameters of the reduction reaction of 4-nitrophenol using NaBH₄ in the presence of p(AAm-co-MTM)-Au catalyst were calculated as $E_a = 38.80$ kJ/mol, $\Delta H^\ddagger = 36.16$ kJ/mol and $\Delta S^\ddagger = -161.37$ J/mol K.

1. Introduction

In recent years metal particles have become frequently used materials due to their high surface-volume ratio. Among these metal particles, gold nanoparticles are of interest because of their use in areas such as optical probes, photocatalysis, optoelectronics and drug delivery systems [1–3]. Gold nanoparticles are indispensable catalysts due to their high catalytic activities at low temperatures. The most important parameter for the use of metal particles as catalyst is the particle size. Although small size particles have high surface area and catalytic activity, they tend to agglomerate due to high surface energies [4]. For this reason, a number of studies have been carried out on the immobilization of metal particles on support materials such as functional polymers [5], nanocrystalline cellulose [6], graphene oxide [7], hydrogels [8–10], phosphazenic microspheres [11,12], fly ash [13] and starch [14] to prevent agglomeration. In the literature, gold nanoparticles supported with materials such as hydrogels have been synthesized [15]. The reduction reaction of p-nitrophenol is generally preferred as the model reaction for examining the catalytic activities of the supported gold particles [16–19].

Nitrophenols, organic pollutants from industrial processes such as the production of explosives, pesticides, plastics and pharmaceuticals, are listed by the USEPA as “Priority Pollutants”. Therefore, the presence of 4-nitrophenol (4-NP) as a toxic chemical in water is an important

environmental issue [20,21]. The most commonly-used method for removing 4-NP from water is to convert it to 4-aminophenol (4-AP) as a result of a catalytic reduction reaction. 4-AP is an important intermediate product of the pharmaceutical industry [22].

Hydrogels, which are crosslinked polymeric networks, may have different swelling and shrinkage behaviors in the aqueous environment due to functional groups in their structures [23]. Thanks to these properties, hydrogels have many applications such as absorption of toxic chemical species, drug release, and separation of ionic species [24–27]. At the same time, hydrogels are a good support material for the synthesis of metal particles. In this work, we synthesized N-metacrylamido thiomorpholine (MTM) monomer containing sulfur atoms in their structure. Then, we prepared co-polymeric hydrogels with different monomer molar ratios of this monomer with acrylamide. We used these thioether functional hydrogels in selective absorption of the Au(III) ion from aqueous medium. We reduced the absorbed gold (III) ions in the hydrogel network structure using NaBH₄ and used the obtained hydrogel-supported gold nanoparticles as a catalyst for the reduction reaction of 4-NP to 4-AP. A series of experiments was carried out, related to the amount of catalyst, the reaction kinetics of 4-NP, and the reusability of catalyst.

* Corresponding author at: Department of Bioengineering, Faculty of Engineering, Canakkale Onsekiz Mart University, Canakkale, Turkey
E-mail address: ozgurozay@comu.edu.tr (O. Ozay).

<https://doi.org/10.1016/j.apcatb.2018.09.066>

Received 18 April 2018; Received in revised form 4 September 2018; Accepted 19 September 2018

Available online 20 September 2018

0926-3373/© 2018 Elsevier B.V. All rights reserved.

2. Experimental

2.1. Reagent and methods

Thiomorpholine (98%), methacryloyl chloride (97%), triethylamine (99%), acrylamide (Aam, 98%), N,N,N',N'-tetramethylethylenediamine (TEMED, 99%), N,N'-methylenebis(acrylamide) (MBA, 99%), NaBH₄ (98%), 4-nitrophenol (4-NP, 99%), ammonium persulfate (APS) and dimethylsulfoxide (DMSO) were purchased from Sigma-Aldrich Chemical Company and used without further purification. Na[AuCl₄] was used as metal ion source. Tetrahydrofuran was dried using Sodium-Benzophenone system. Deionized water was used during all studies.

The FT-IR spectra of monomer and hydrogel were recorded by a Perkin Elmer FT-IR instrument using ATR apparatus at 4000–650 cm⁻¹. All UV–vis measurements were carried out using PG Instrument T80 + UV–vis Spectrophotometer for catalytic investigation. NMR spectra of N-Methacrylamidothiomorpholine (MTM) monomer were recorded by JEOL NMR-400 MHz instrument using CDCl₃ as solvent and Tetramethylsilane (TMS) as internal standard. The morphology of hydrogel and hydrogel-Au composite were monitored by scanning electron microscopy (SEM, JEOL-SEM). Also, the chemical compositions of materials were analyzed using the energy dispersive X-Ray analysis. The transmission electron microscope (TEM) analysis was performed with a JEOL TEM-1400 electron microscope operating at 50 kV. X-Ray diffraction (XRD) analysis of hydrogel and hydrogel-Au composite was carried out using PANalytical Empyrean instrument at a wide-angle range. The metal amount in the hydrogel-Au composite was determined using ICP-OES.

2.2. Synthesis of N-methacrylamido thiomorpholine (MTM)

The solution of methacryloylchloride (5.38 g; 50 mmol) in dry THF (100 ml) was added dropwise to the solution of thiomorpholine (5.16 g; 50 mmol) and triethylamine (7.60 g; 75 mmol) in dry THF (200 ml) for 2 h at 0 °C under argon atmosphere. At the end of this time, the reaction mixture was filtered to separate the formed triethylammonium chloride salts. The solid was washed with dry THF (50 ml). The solvent of filtrate was removed under reduced pressure. The yellow oily residue was separated using column chromatography with silica gel as filler and CHCl₃:hexane (1:1) solvent mixture as eluent. MTM was obtained as colorless oil (7.27 g, 85% yield). FT-IR (ν_{max} , cm⁻¹): 2928–2835 (CH), 1619 (C=O). ¹H NMR (400 MHz, CDCl₃, ppm): 5.13 (1H, s), 4.97 (1H, s), 3.77 (4H, m, –N–CH₂–), 2.57 (4H, m, –S–CH₂–), 1.89 (3H, s, –CH₃). ¹³C NMR (100 MHz, CDCl₃, ppm): 18.3, 28.2, 45.9, 123.9, 141.7, 171.2. Anal. Calcd for C₈H₁₃NOS: C, 56.11; H, 7.65; N, 8.18; S, 18.72. Found: C, 55.98; H, 7.69; N, 8.11, 18.34.

2.3. Preparation of p(AAm-co-MTM) hydrogels

The synthesis of p(AAm-co-MTM) hydrogels with different monomer mole ratios were carried out as a result of the free radical polymerization reaction of AAm with MTM in the presence of MBA as crosslinker. The amounts of reagents used for the synthesis of AAm-co-

MTM hydrogels are summarized in Table 1. Briefly, AAm, MTM and MBA at amounts given in Table 1 were dissolved in DMSO and 50 μ l TEMED was added to solution. Then, 100 μ l volume of the initiator solution in deionized water (1% with respect to total monomer mole) was added to the reaction mixture. The mixture was rapidly stirred to obtain a homogeneous solution. Then, the mixture was injected into plastic pipettes with an injector. The pipettes were maintained at room temperature for 12 h to complete the polymerization reaction. At the end of this time, the hydrogels were removed from pipettes and cut into 5 mm long cylinders. The hydrogels were firstly washed with DMSO for 24 h to remove unreacted monomers. Then, the hydrogels were washed with deionized water for 48 h. The cleaned hydrogels were dried in a vacuum oven at 40 °C and were packed for use in catalyst applications.

2.4. Swelling characterization of hydrogels

The synthesis yields of the p(AAm-co-MTM) hydrogels that were prepared as a series with the redox polymerization technique were determined in a gravimetric manner as follows: At the end of the synthesis, the hydrogel that was removed from the pipette as a whole was washed with deionized water for 2 days to remove the monomers, crosslinkers and other chemical species that did not react. Then the mass of the dried hydrogel was determined.

The water retention amounts of the dry p(AAm-co-MTM) hydrogels by mass were determined by using Eq. (1) after swelling in deionized water.

$$\text{Swelling (\%)} = [(M_s - M_d)/M_d] \times 100 \quad (1)$$

The M_d and M_s given in the equation are the mass of the dry hydrogel and the mass of the swollen hydrogel measured at specific times, respectively.

2.5. Preparation of p(AAm-co-MTM) hydrogel-supported gold nanoparticle

For the purpose of preparing gold nanoparticles in the network structures of the P(AAm-co-MTM) hydrogels, 30 mg hydrogel was kept in 100 ppm (50 ml) gold(III) solution for 12 h. After this time, the hydrogel was washed with deionized water and transferred to 0.5 M 50 ml NaBH₄ solution and was kept in it for 2 h. The obtained hydrogel-metal composites were used for characterization and catalysis experiments. The experiments for selective metal ion absorption of the hydrogels were performed in a mixture that had 50 ml 100 ppm Co (II), Ni(II), Cu (II) and Au(III) by using 30 mg hydrogel. The amounts of the metal ions absorbed by hydrogels were measured from the absorption solution with ICP-OES.

2.6. Catalytic reduction of 4-NP

The catalytic reduction reaction of 4-NP was carried out in the presence of p(AAm-co-MTM)-Au catalyst using NaBH₄ as reducing agent in aqueous media. Briefly, 50 ml of 10 mM 4-NP solution in deionized water was added to a two-necked round bottom reaction flask. Then, solid NaBH₄ (with a final concentration of 100 mM) and catalyst were added to the magnetically-stirred solution of 4-NP at

Table 1

The synthesis conditions of p(AAm-co-MTM) hydrogels.

Hydrogel Code	AAm (mmol)	MTM (mmol)	Monomer Feed Ratio	MBA (%)	TEMED (μ l)	DMSO (ml)
Hydrogel1	40	–	100:0	0.25	50	2
Hydrogel2	38	2	95:5	0.25	50	2
Hydrogel3	36	4	90:10	0.1	50	2
Hydrogel4	32	8	80:20	0.25	50	2
Hydrogel5	36	4	90:10	0.25	50	2
Hydrogel6	36	4	90:10	0.5	50	2
Hydrogel7	36	4	90:10	0.75	50	2

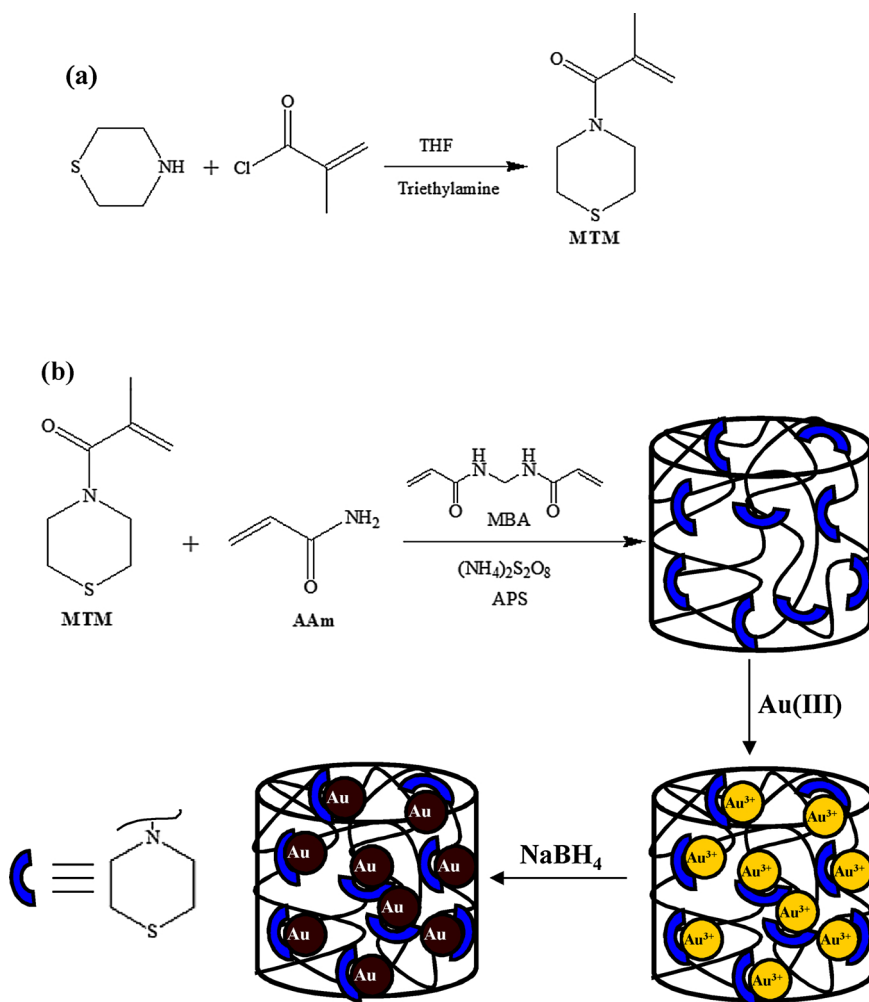


Fig. 1. Schematic representation of the synthesis of (a) MTM monomer and (b) Hydrogel5 and Hydrogel5-Au catalyst.

constant temperature (30–60 °C). The reduction of 4-NP to 4-AP was monitored using UV–vis spectrophotometer by recording the spectra of samples taken at certain intervals from the reaction media. UV–vis spectra of the samples were recorded in the range of $\lambda = 200\text{--}600\text{ nm}$ at ambient temperature.

3. Results and discussion

3.1. Preparation and characterization of p(AAm-co-MTM)-Au catalyst

The surface modification of gold nanoparticles is especially important to increase functionality in biomedical applications [17]. For this purpose, many studies have been conducted in recent years on the synthesis of gold nanoparticles whose surfaces are modified with organic thiols [28,29]. Since the Au-S bonding is strong, it is extremely difficult to remove the thiol groups from the surface of the gold. Although this situation has several disadvantages in practice, thiol or thioether groups have valuable advantages like enabling the selected absorption of gold ions with the help of this strong bonding feature [30–33]. In addition, studies have been performed in recent years showing that removing thiolate ligands from the surface of gold is possible by using excessive NaBH₄. In this way, attempts have been made to eliminate the disadvantages stemming from the removal of thiol groups from the surface of the gold [34,35]. Since Au-S bonding is strong, thiols or thioether groups have been used as good anchoring groups in preparing gold nanoparticles [28–35]. For this reason, in our present study, we performed the synthesis of a new type of hydrogel

that included thioether groups which might allow the selective absorption of gold(III) ions from aqueous media. For this purpose, we synthesized the MTM monomer from the reaction of thiomorpholine with methacryloyl chloride (Fig. 1(a)). The structural characterization of the monomer was performed (Figs. S1–S4). Then, we prepared the p(AAm-co-MTM) hydrogels in the presence of MBA as a crosslinker with the redox polymerization of the AAm and MTM (Fig. 1(b)). The swelling properties of the prepared hydrogels were examined. Hydrogels are three-dimensional polymers with linear polymeric chains binding to each other with crosslinks. This chemical structure ensures that hydrogels are swollen without dissolving in water. The water retention properties of hydrogels diversify their usage areas. In the scope of the present study, the synthesis yield and water retention capacities of the p(AAm-co-MTM) hydrogels synthesized as a series are given in Fig. 2. The p(AAm-co-MTM) hydrogels to be used as catalyst support material were synthesized to include 0%, 5%, 10% and 20% MTM by mole ratio as shown in Table 1. In addition, the hydrogels were synthesized by using four different crosslinker ratios (0.1%, 0.25%, 0.5% and 0.75% MBA). As shown in Fig. 2(a), while the p(AAm) hydrogel that contains 0.25% MBA synthesized with 93% yield retains 741% water by mass, adding MTM to the structure of the hydrogel reduces the synthesis yield, although it increases the water retention amount of hydrogels. In this respect, when MTM is added to the structure of 0.25% crosslinked copolymeric hydrogel at 0%, 5%, 10% and 20% molar ratios, water retention capacities become 792%, 845% and 993%, respectively. The yields of these reactions were determined as 88%, 79% and 73%, respectively. Among all the hydrogels synthesized, the most ideal one in

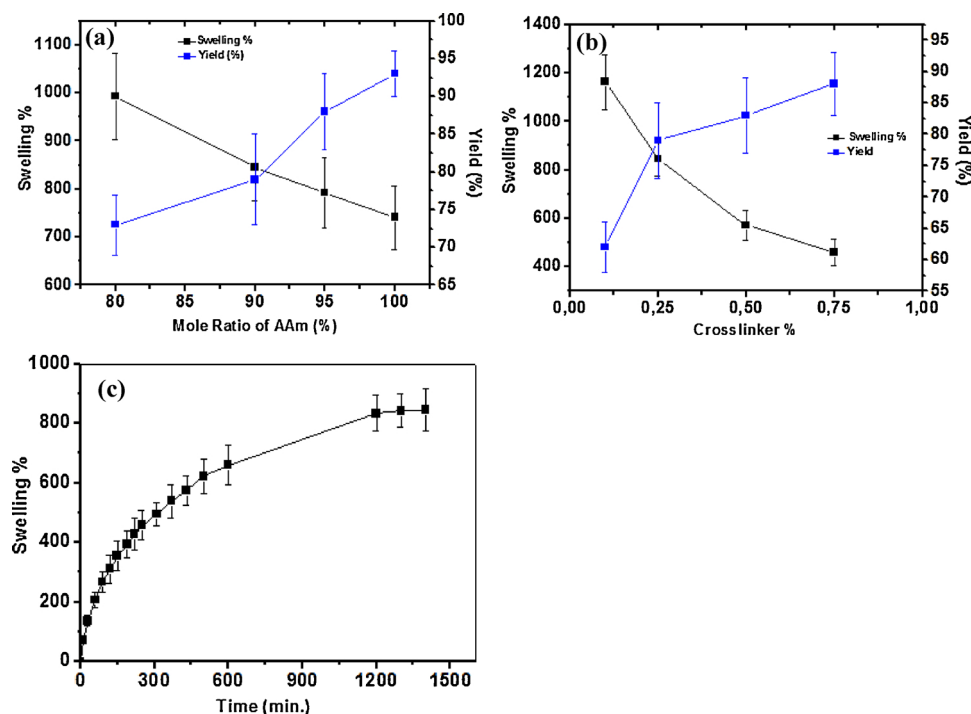


Fig. 2. Swelling properties and polymerization yield of (a) p(AAm-co-MTM) hydrogels with different mole ratio of AAm, (b) p(AAm-co-MTM) hydrogels with different crosslinker ratio and (c) swelling properties of **Hydrogel5**.

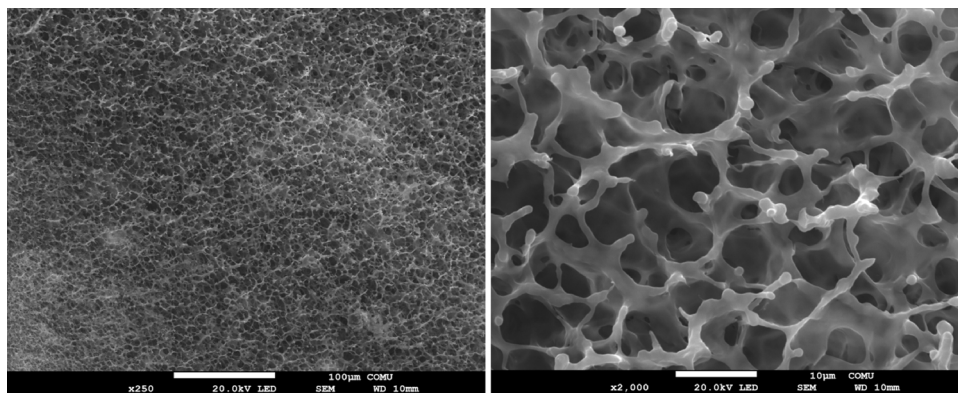


Fig. 3. SEM images of **Hydrogel5**.

Table 2

The amount of absorbed metal ion by **Hydrogel5**.

Solution Content	Initial Concentration (ppm)	Last Concentration (ppm)	Absorption (mg/g)
Co (II)	100	98.6	2.33
Ni (II)	100	98.9	1.83
Cu (II)	100	99.3	1.16
Au (III)	100	48.2	80.25

(50 ml, 100 ppm, 30 mg hydrogel 5).

terms of water retention capacity, MTM ratio, synthesis yield and physical properties was **Hydrogel5**. In addition, the effects of cross-linking ratio on the reaction yield and water retention capacity of p(AAm-coMTM) hydrogels containing 10% mole ratio of MTM was investigated. The reaction yield and water retention capacity values of hydrogels containing 10% mole ratio of MTM and 0.1%, 0.25%, 0.50% and 0.75% crosslinker according to total monomer mole are given in Fig. 2(b). According to Fig. 2(b), increasing the crosslink ratio to 0.75% from 0.1% reduces the water retention capacity of the hydrogel;

however, it increases the reaction yield. In this respect, while 0.1% crosslinked **Hydrogel3** retained water at a ratio of 1163% by mass, these ratios were 845%, 572% and 460% for **Hydrogel5**, **Hydrogel6** and **Hydrogel7**. The synthesis yields for these hydrogels are 62%, 79%, 83% and 88%, respectively. The swelling kinetics depending on time for **Hydrogel5**, that was selected to be used as catalyst support material and for ion absorption from the aqueous solution of Au(III), are given in Fig. 2(c). When Fig. 2(c) is examined, it is seen that **Hydrogel5** reaches the balance swelling position in approximately 1000 min.

The porous structure of the p(AAm-co-MTM) hydrogels to be used as catalyst support material is extremely important for the diffusion of the reactives into hydrogels in the reaction medium. The SEM images of **Hydrogel5** were taken after freeze-drying the swollen hydrogels and are shown in Fig. 3. As seen in Fig. 3, hydrogels have an extremely porous structure. In addition, the sizes of the pores are distributed almost homogeneously throughout the hydrogel. The size of the pores is approximately 10 µm. The amount of gold(III) ions absorbed by **Hydrogel5**, that includes selective sulfur atoms for gold ions (III) in its structure, was determined as 83.7 mg Au(III)/g dry hydrogel with ICP-OES. In addition, the amounts of metal ions adsorbed by **Hydrogel5**

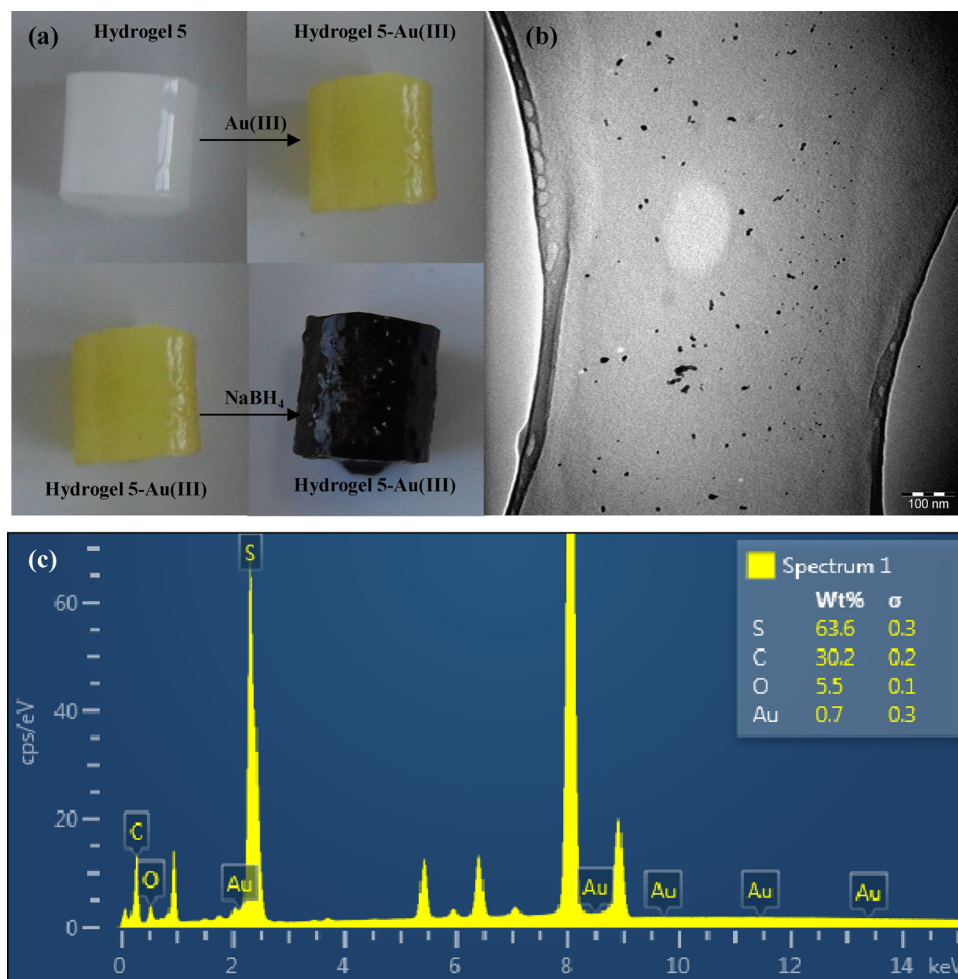


Fig. 4. (a) Digital camera images of **Hydrogel5**, **Hydrogel5-Au(III)** and **Hydrogel5-Au**, (b) TEM images (c) EDX spectrum of **Hydrogel5-Au** composite catalyst.

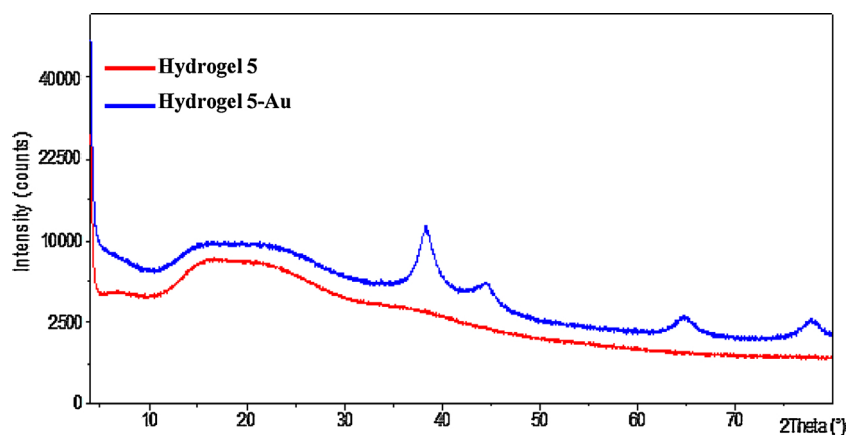


Fig. 5. XRD pattern of **Hydrogel5** and **Hydrogel5-Au** composite catalyst.

from 50 ml of solution containing 100 ppm Co(II), Ni(II), Cu(II) and Au (III) ions are given in Table 2. According to the absorption values obtained, it can be said that hydrogels are selective for Au(III) ions in the mixed medium. With this property, p(AAm-co-MTM) hydrogels act as selective catalyst support material. The digital camera image of the **Hydrogel5-Au** composite catalyst obtained as a result of the reduction of Au(III) ions absorbed from the single medium by **Hydrogel5** with NaBH_4 is given in Fig. 4 (a); and the TEM image is given in Fig. 4 (b). As seen in the figure, the gold particles are diffused almost homogeneously in the network structure of the hydrogel to be used as support material.

The size of the gold nanoparticles is approximately 10–20 nm range. In addition, the observation of the peak for gold metal in the TEM-EDX image (Fig. 4(c)) of the **Hydrogel5-Au** composite catalyst is important evidence for the fact that Au(III) ions were absorbed by p(AAm-co-MTM) hydrogels and that the absorbed Au(III) ions were successfully reduced.

The XRD patterns of **Hydrogel5** and **Hydrogel5-Au** composite catalyst are given in Fig. 5. The fact that **Hydrogel5** has an amorphous structure is understood from the wide peak in 2θ angle in the XRD pattern in 10–30° range. A similar peak is also seen in the same area of

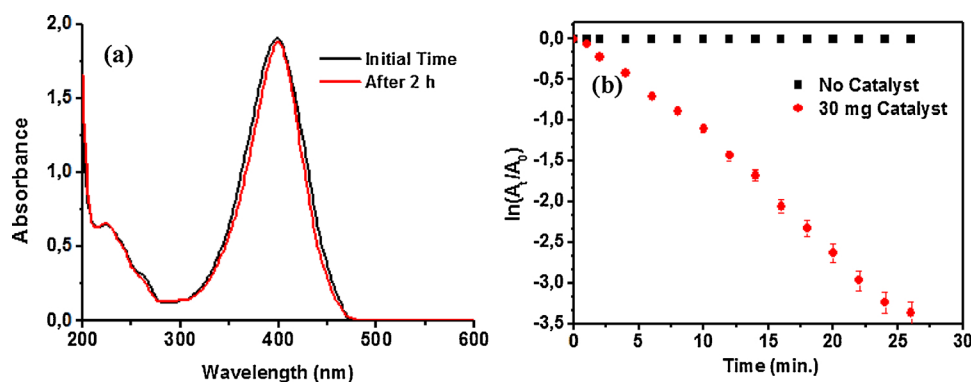


Fig. 6. (a) UV-vis spectra of control experiments and (b) $\ln(A_t/A_0)$ -t plot in the presence and absence of **Hydrogel5-Au** composite catalyst.

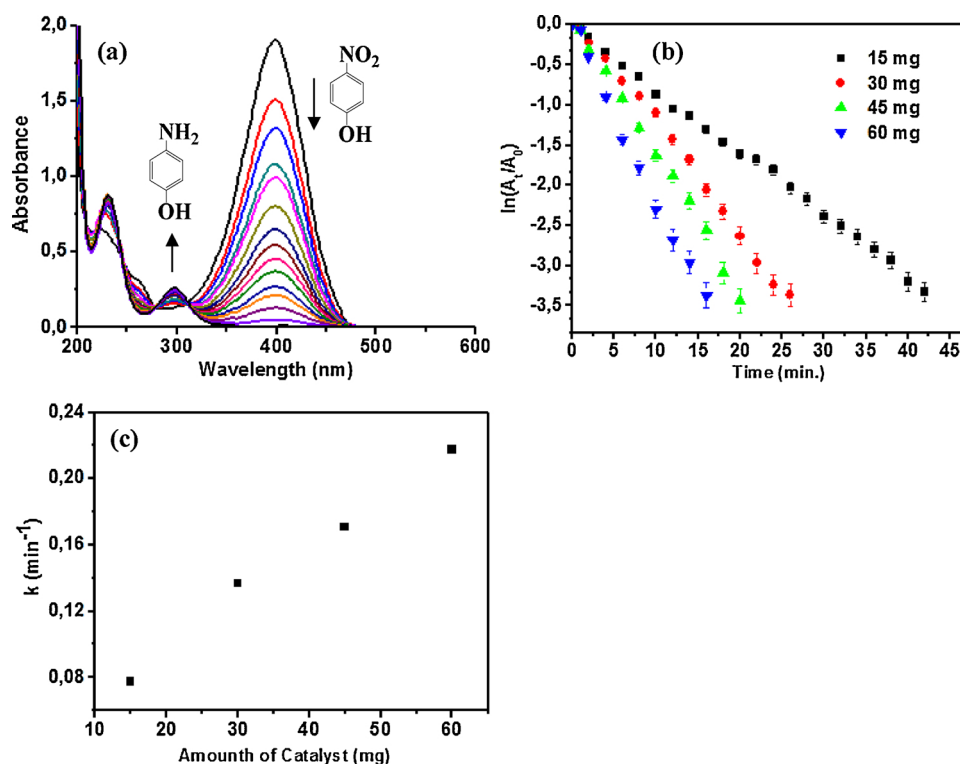


Fig. 7. (a) UV-vis spectra of the reduction reaction of 4-NP (10 mM) in the presence of NaBH_4 (100 mM) and **Hydrogel5-Au** composite catalyst (30 mg; containing 2.50 mg Au) at 30 °C, (b) The $\ln(A_t/A_0)$ plot versus time in the presence different amounts of catalyst and (c) the change of k_{app} with catalyst amount.

the XRD pattern of the **Hydrogel5-Au** composite catalyst. The XRD pattern of the **Hydrogel5-Au** composite catalyst also contains sharp peaks at 2θ angles of 38.5° , 44.4° , 64.8° and 77.6° . These peaks correspond to the (111), (200), (220) and (311) crystal planes of the surface-centered cubic (FCC) gold [11,36,37]. These results support the presence of gold nanoparticles in the network structure of **Hydrogel5** and these gold nanoparticles have crystalline structure.

3.2. Catalytic properties of *p*(AAm-co-MTM)-Au composite catalyst

For the purpose of examining the catalytic activity of **Hydrogel 5-Au** composite material, the reduction reaction of 4-NP to 4-AP in the presence of NaBH_4 was chosen as the model reaction. The reduction reaction of 4-NP by NaBH_4 in the presence of **Hydrogel5-Au** (containing 2.50 mg Au) composite catalyst was monitored by using UV-vis spectroscopy. Excessive NaBH_4 was used in the reaction. 4-NP has an absorption band at $\lambda = 317$ nm for pH values that are close to neutral. The fact that the absorbance value of 4-NP shifted to $\lambda = 400$ nm with the addition of NaBH_4 to the aqueous solution of 4-NP is seen easily in

Fig. 6(a). It is also possible to see this shift in the wavelength in the change of the color of the reaction medium into bright yellow from colorless. The reason for this change in absorption wavelength is that the pH of the reaction medium is increased above 10 by the addition of NaBH_4 . In this way, 4-NP is deprotonated and 4-nitrophenolate forms in the reaction media [12]. Firstly, the reduction reaction of 4-NP with NaBH_4 in the absence of catalyst was examined. No significant change was observed in the absorbance intensity of 4-nitrophenolate at $\lambda = 400$ nm or in peak position in the absence of catalyst even at the end of 2 h (Fig. 6(a) and (b)). In all catalytic experiments, in order to overcome the time delay problem, the oxygen in the solution is removed by passing argon gas through the 4-NP solution before the reactions are started. It was observed that the absorbance at $\lambda = 400$ nm decreased in time with the addition of **Hydrogel5-Au** composite catalyst to the reaction mixture that included 4-NP and NaBH_4 (Fig. 7(a)). In addition, with the progression of the reaction, the bright yellow color of the reaction medium changed to colorless. Simultaneous with the decrease in absorbance at $\lambda = 400$ nm, a new peak emerged at $\lambda = 298$ nm. This peak with intensity increasing throughout the

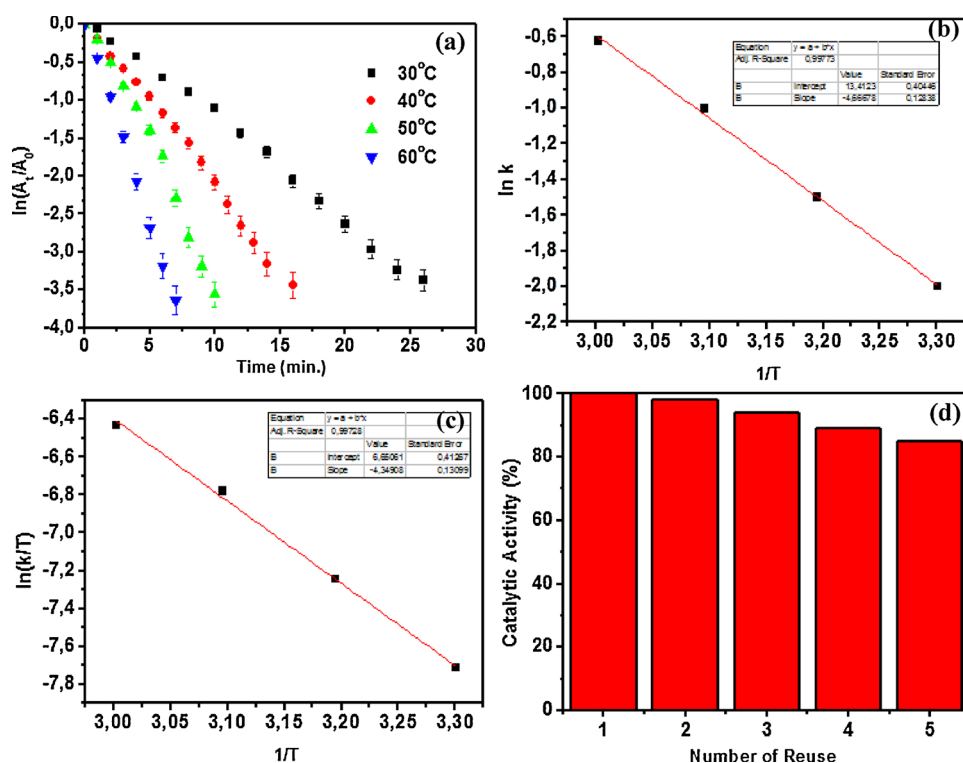


Fig. 8. (a) The $\ln(A_t/A_0)$ plot versus time in the presence of NaBH_4 (100 mM) and **Hydrogel5-Au** composite catalyst (30 mg; containing 2.50 mg Au) at different temperature, (b) Arrhenius plot, (c) Eyring plot of the catalytic reduction of 4-NP and (d) reusability of **Hydrogel5-Au** composite catalyst (30 mg; containing 2.50 mg Au).

Table 3

The rate constants and TOF values of metal particles used for the catalytic reduction of 4-NP.

Catalyst	$k_{app}(\text{s}^{-1})$	TOF (h^{-1})	Refs.
Pd/MFCNC	5.83×10^{-3}	3168	[4]
CNCs-Au	1.47×10^{-2}	641	[6]
PCP@Au-Ag	2.87×10^{-3}	130	[11]
PAM/PPY/GO-Ag	2.10×10^{-2}	153.42	[46]
Au/graphene hydrogel	3.17×10^{-3}	12	[47]
HPGNPs	7.47×10^{-3}	94	[48]
PS/Au	1.88×10^{-3}	–	[20]
Chitosan/Au	2.60×10^{-3}	–	[15]
PVP/Au	1.17×10^{-3}	–	[31]
Dodecanthiol/Au	0.93×10^{-3}	–	[31]
p(AAm-co-TMT)@Au	2.30×10^{-3}	322.89	This work

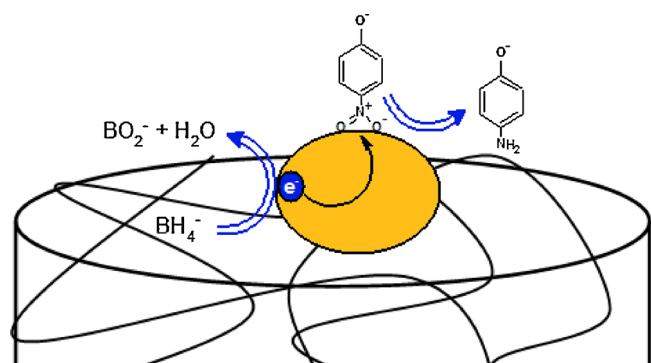


Fig. 9. Purposed mechanism of the reduction of 4-NP in the presence of **Hydrogel5-Au** composite catalyst.

reaction is the absorption peak for 4-AP [1,3].

In the reduction reaction of 4-NP, the excess amount of NaBH_4 according to 4-NP was used. The apparent rate constant (k_{app}) values were computed from the following equation;

$$\ln(C_t/C_0) = \ln(A_t/A_0) = -k_{app}t$$

Here, C_t and A_t refer to the concentration of 4-NP at t time, and the absorbance value at $\lambda = 400$ nm; C_0 and A_0 refer to the initial concentration of 4-NP and absorbance value. The rate constant k_{app} was calculated from the $\ln(A_t/A_0)$ graphics drawn against time by using this equation [38].

In order to determine the effect of the catalyst amount on the reduction reaction, a serial reaction was performed at 30 °C in the presence of catalyst with changing amounts while keeping the 4-NP and NaBH_4 concentrations stable. When the rate constants obtained from the $\ln(A_t/A_0)$ -time graphics given in Fig. 7(b) are examined (Fig. 7(c)), it is seen that there is a linear increase in the k_{app} values of the 4-NP reduction reaction with the increase in catalyst amount.

One of the most important parameters in examining the activity of a new catalyst is the activation energy (E_a). For this reason, the reduction reaction of 4-NP with NaBH_4 was performed at four different temperatures (30, 40, 50, 60 °C) in the presence of **Hydrogel5-Au** composite catalyst. An $\ln(A_t/A_0)$ graphic was formed against time for each temperature. The k_{app} values were calculated from the slope of these graphs, given in Fig. 8(a), as 0.1355, 0.2234, 0.3666 and 0.5358 min^{-1} for 30, 40, 50, 60 °C, respectively. The activation energy of the reaction E_a , activation enthalpy ΔH^\ddagger and activation entropy ΔS^\ddagger were calculated from the curves given in Fig. 8(b) and (c) that were formed according to the Arrhenius and Eyring equations [12,13]. The $E_a = 38.80$ kJ/mol of the reduction reaction of 4-NP in the presence of **Hydrogel5-Au** composite catalyst identified $\Delta H^\ddagger = 36.16$ kJ/mol and $\Delta S^\ddagger = -161.37$ J/mol K. In addition, the Turnover Frequency (TOF) of the p(AAm-co-TMT)-Au composite catalyst was determined as 322.89 h^{-1} [4]. The TOF and rate constant values reported in the literature for the catalytic reduction reaction of 4-NP are summarized in Table 3. As seen in Table 3, the rate constant value of **Hydrogel5-Au** composite catalyst is comparable with the earlier report for the gold catalyst. However, our catalyst system is superior to some of the different composite catalysts reported in the literature for the reduction reaction of 4-NP. For example, the rate constant was reported as 0.010 min^{-1} for Au@Pt nanoflowers [39]. It was reported that the k_{app} value of the reduction

reaction of 4-NP in the presence of water-washed fly ash supported Fe nanoparticles as catalyst was 0.043 min^{-1} [40]. Similarly, k_{app} is reported as 0.075 min^{-1} for $\text{CoFe}_2\text{O}_4/\text{GQD}$ catalyst [41]; as $3.3 \times 10^{-2} \text{ min}^{-1}$ for Peptide-Based Hydrogel supported Ag nanoparticles [42]; as 0.134 min^{-1} for Ag-nanoparticle embedded p(AA) hydrogel [43]; as 0.0563 min^{-1} for hydrogel supported Ni nanoparticles [9], and as 0.12 min^{-1} for hydrogel supported Co nanoparticles [10]. The E_a value found complies with the E_a values reported before for the catalytic reduction reaction of 4-NP. In the study conducted by Liu et al. in which protein-directed gold nanoparticles were used as catalyst, the E_a value was reported as 13.47 kJ/mol [44]. Similarly, it was reported that the E_a value of the reaction was 33.6 kJ/mol [45] when hollow porous gold nanoparticles were used as catalyst. Jiong et al. reported the activation energy of the reduction reaction of 4-NP catalyzed by hierarchical copper nanoparticles as 34.8 kJ/mol [48]. However, there are also some other studies in the literature reporting E_a values over 40 kJ/mol . For example, E_a is reported as 47.42 kJ/mol for starch-supported gold nanoparticles [14]; as 40.25 kJ/mol for Ag nanoparticles [49]; as 51.30 kJ/mol for meso-Co-150 catalyst [50], and as 68.60 kJ/mol for silver-absorbed waste nanocomposite [51]. In the light of this information, it can be said that **Hydrogel5-Au** composite system is a good candidate as catalyst for the reduction of 4-NP.

In addition to the activity in catalytic reactions, another important parameter is the reusability of the catalyst. The steadier a heterogeneous catalyst acts in a reaction medium, the more reusability it has for the same reaction. This feature makes the catalyst economically good. For this reason, the reusability of **Hydrogel5-Au** composite catalyst in the reduction reaction of 4-NP was examined. For this purpose, the same catalyst was used five successive times in the reduction reaction of 4-NP in the presence of NaBH_4 at 30°C . After five uses, the reaction yield did not change and a 15% reduction was determined in the activity of the catalyst (Fig. 8(d)). This slight decrease observed in the activity of the catalyst may be attributed to small mass losses during washing and reuse process [2,19], the adsorption of the reaction product (4-AP) and the borates formed as a result of the hydrolysis of NaBH_4 to the gold nanoparticle surface [37,52] and the poisoning of the catalyst by oxidation which reduces the activity of the gold centers in the catalyst [14,53]. Gold, which has excellent activity as a catalyst, is very valuable because of its rarity on the earth. Therefore, the regeneration of deactivated gold catalysts is highly desirable. For this purpose, the techniques such as cold plasma regeneration [54], square-wave pulse plasma [55] and redispersion [56] have been used for the regeneration of deactivated gold catalyst in the literature. Currently, Ruan et al. reported a efficiently regeneration of deactivated Au/C catalyst using dispersion method for the reduction reaction of 4-NP [56]. However, new studies on regeneration of gold nanoparticles supported with different materials should be made. In the future, our group will focus on the reactivation of gold particles supported by polymeric materials. Since one of the targets of this present study was to prepare selective support material, the Au(III) ions absorbed by **Hydrogel5** from the metal ion mixture were reduced by using NaBH_4 . The **Hydrogel5-Au** composite catalyst obtained in this way was used in the reduction reaction of 4-NP. While the rate constant $k_{\text{app}} = 0.1355 \text{ min}^{-1}$ of the catalyst was obtained as a result of the absorption of Au(III) ions from single ion media at 30°C , the rate constant of the catalyst obtained as a result of the absorption of Au(III) ions from the multiple metal ion media under the same conditions was determined as $k_{\text{app}} = 0.1337 \text{ min}^{-1}$.

In investigating the catalytic activity of a newly-developed catalyst, the reduction reaction of 4-NP to 4-AP is frequently used as the model reaction. In many previous studies, a mechanism that was based on Langmuir-Hinshelwood mechanism was recommended. NaBH_4 is a strong reducing agent because of its low standard redox potential ($-1.2 \text{ E}^\circ/\text{V}$ at $\text{pH} = 14$). BH_4^- is an ion loaded negatively and because of the repulsion between the 4-nitrophenolate anion and BH_4^- in the alkali reaction medium that occurs with the addition of NaBH_4 the reduction

reaction does not occur in the absence of catalyst. However, when a metallic heterogeneous catalyst exists in the medium, the reaction starts to proceed. Here, the factor which ensures that the reaction happens is the chemisorption of BH_4^- and the anchoring of 4-nitrophenolate anion to the surface of the catalyst by using nitro group. After these bindings, the reduction reaction occurs at the catalyst surface, and following it, 4-AP leaves the catalyst surface [57]. In the light of this information, the mechanism of the reduction reaction of 4-NP in the presence of **Hydrogel5-Au** composite catalyst is recommended in Fig. 9.

4. Conclusion

In the literature metal catalysts supported with various different materials have been prepared for the reduction of aromatic nitro compounds. However, studies on metal ion selective support materials are extremely limited. As known, the sulfur atom can act as a selective donor atom for gold ions. Therefore, we synthesized a support material that showed selective features for Au(III) ions in our present study. For this purpose, we prepared MTM monomer, which is a thioether derivative. By using this monomer, we synthesized copolymeric **Hydrogel5**. We examined the absorption behavior of **Hydrogel5** in metal ion mixture, and in the end, we determined that **Hydrogel5** selectively absorbed Au(III) ions. In this way, after we prepared the selective support material we targeted, we synthesized gold nanoparticles by using this support material. Then, we used **Hydrogel5-Au** composite material as a catalyst in the reduction reaction of 4-NP and determined that **Hydrogel5-Au** composite had good catalytic activity. As a result of the experiments performed at four different temperatures in the presence of **Hydrogel5-Au** catalyst, we determined the activation parameters of the reduction reaction of 4-NP as $E_a = 38.80 \text{ kJ/mol}$, $\Delta H^\ddagger = 36.16 \text{ kJ/mol}$ and $\Delta S^\ddagger = -161.37 \text{ J/mol K}$. Thus, we performed the synthesis, characterization and catalytic application of a new support material that enabled select Au(III) absorption and supported synthesis of gold nanoparticles as a result of the reduction of absorbed Au(III) ions.

Appendix A. Supplementary data

Supplementary material related to this article can be found, in the online version, at doi: <https://doi.org/10.1016/j.apcatb.2018.09.066>.

References

- [1] Z. Yana, L. Fua, X. Zuoa, H. Yang, Appl. Catal. B: Environ. 226 (2018) 23–30.
- [2] M. Li, X. Li, X. Qi, F. Luo, G. He, Langmuir 31 (2015) 5190–5197.
- [3] J. Hwang, A.B. Siddique, Y.J. Kim, H. Lee, J.H. Maeng, Y. Ahn, J.S. Lee, H.S. Kim, H. Lee, RSC Adv. 8 (2018) 1758–1763.
- [4] X. Wu, Z. Shi, S. Fu, J. Chen, R.M. Berry, K.C. Tam, Strategy for synthesizing porous cellulose nanocrystal supported metal nanocatalysts, ACS Sust. Chem. Eng. 4 (2016) 5929–5935.
- [5] H. Amari, M. Guerrouache, S. Mahouche-Chergui, R. Abderrahim, B. Carbonnier, React. Funct. Polym. 121 (2017) 58–66.
- [6] W. Yan, C. Chen, L. Wang, D. Zhang, A.J. Lid, Z. Yao, L.Y. Shi, Carbohydr. Polym. 140 (2016) 66–73.
- [7] M. Cao, L. Feng, P. Yang, H. Wang, X. Liang, X. Chen, J. Mater. Sci. 53 (2018) 4874–4883.
- [8] H. Ozay, O. Sahin, O.K. Koc, O. Ozay, J. Indust. Eng. Chem. 43 (2016) 28–35.
- [9] N. Sahiner, H. Ozay, O. Ozay, N. Aktas, Appl. Catal. A: General 385 (2010) 201–207.
- [10] N. Sahiner, H. Ozay, O. Ozay, N. Aktas, Appl. Catal. B: Environ. 101 (2010) 137–143.
- [11] J. Fu, S. Wang, J. Zhu, K. Wang, M. Gao, X. Wang, Q. Xu, Mater. Chem. Phys. 207 (2018) 315–324.
- [12] O. Sahin, O.K. Koc, H. Ozay, O. Ozay, J. Inorg. Organomet. Polym. Mater. 27 (2017) 122–130.
- [13] H. Ozay, Sci. Adv. Mater. 5 (6) (2013) 575–582.
- [14] S. Chairam, W. Konkamdee, R. Parakhun, J. Saudi Chem. Soc. 21 (2017) 656–663.
- [15] X.Q. Wu, X.W. Wu, Q. Huang, J.S. Shena, H.W. Zhang, Appl. Surf. Sci. 331 (2015) 210–218.
- [16] J. Liu, Q. Chen, Y.N. Sun, M.Y. Xu, W. Liu, B.H. Han, RSC Adv. 6 (2016) 48543.
- [17] S.M. Ansar, C.L. Kitchens, ACS Catal. 6 (2016) 5553–5560.
- [18] Z. Zhang, G. Sèbea, X. Wang, K.C. Tam, Carbohydr. Polym. 182 (2018) 61–68.

- [19] Md. T. Islama, N. Dominguez, Md. A. Ahsana, H. Dominguez-Cisnerosa, P. Zunigac, P.J.J. Alvarez, J.C. Noveron, *J. Environ. Chem. Eng.* 5 (2017) 4185–4193.
- [20] Y. Zhao, Z. Wu, Y. Wang, C. Yang, Y. Li, *Colloids surf. A Physicochem. Eng. Asp.* 529 (2017) 417–424.
- [21] S. Kundu, A. Chanda, J.V.K. Thompson, G. Diabes, S.K. Khetan, A.D. Ryabov, T.J. Collins, *Catal. Sci. Technol.* 5 (2015) 1775–1782.
- [22] Z. Hasan, D.W. Cho, C.M. Chon, K. Yoon, H. Song, *Chem. Eng. J.* 298 (2016) 183–190.
- [23] P. Ilgin, O.S. Zorer, O. Ozay, G. Boran, *J. Appl. Polym. Sci.* 134 (2017) 45550.
- [24] H. Ozay, O. Ozay, *J. Macromol. Sci. Part A Pure Appl. Chem.* 51 (2014) 308–317.
- [25] O. Ozay, *J. Appl. Polym. Sci.* 131 (2014) 39660.
- [26] H. Ozay, O. Ozay, *Chem. Eng. J.* 232 (2013) 364–371.
- [27] N. Sahiner, O. Ozay, N. Aktas, *Chemosphere* 85 (2011) 832–838.
- [28] E. Leary, L.A. Zotti, D. Miguel, I.R. Márquez, L. Palomino-Ruiz, J.M. Cuerva, G. Rubio-Bollinger, M.T. González, N. Agrait, *J. Phys. Chem. C* 122 (6) (2018) 3211–3218.
- [29] S.M. Ansar, G.S. Perera, D. Jiang, R.A. Holler, D. Zhang, *J. Phys. Chem. C* 117 (17) (2013) 8793–8798.
- [30] S. Athukorale, M. De Silva, A. LaCour, G.S. Perera, C.U. Pittman Jr., D. Zhang, *J. Phys. Chem. C* 122 (4) (2018) 2137–2144.
- [31] Y. Fu, Y. Lu, F. Polzer, M. Ch. Lux-Steiner, C.H. Fischer, *Adv. Synth. Catal.* 358 (2016) 1440–1448.
- [32] P. Scholder, M. Hafner, A.W. Hassel, I. Nischang, *Eur. J. Inorg. Chem.* 7 (2016) 951–955.
- [33] Y. Xu, T. Wang, Z. He, A. Zhong, K. Huang, *Microporous Mesoporous Mater.* 229 (2016) 1–7.
- [34] S.M. Ansar, F.S. Ameer, W. Hu, S. Zou, C.U. Pittman Jr., D. Zhang, *Nano Lett. (Lett.)* 13 (3) (2013) 1226–1229.
- [35] S.M. Ansar, G.S. Perera, F.S. Ameer, S. Zou, C.U. Pittman Jr., D. Zhang, *J. Phys. Chem. C* 117 (26) (2013) 13722–13729.
- [36] J. Gong, *Chem. Rev.* 112 (5) (2012) 2987–3054.
- [37] Z. Wu, L. Wang, Y. Hu, Y. Li, *Coll. Polym. Sci.* 294 (7) (2016) 1165–1172.
- [38] M.J.S. Mohamed, K.B. Denthaje, *Ind. Eng. Chem. Res.* 55 (27) (2016) 7267–7272.
- [39] D.A. Jency, R. Parimaladevi, A.J. Amali, G.V. Sathe, M. Umadevi, *Colloids Surf. A Physicochem. Eng. Asp.* 554 (2018) 218–226.
- [40] J. Park, S. Bae, *Chemosphere* 202 (2018) 733–741.
- [41] Z. Naghshbandi, N. Arsalani, M.S. Zakerhamidi, K.E. Geckeler, *Appl. Surf. Sci.* 443 (2018) 484–491.
- [42] S. Paul, K. Basu, K.S. Das, A. Banerjee, *ChemNanoMat* 4 (2018) 882–887.
- [43] M. Ghorbanloo, A. Heydari, H. Yahiro, *Appl. Organometal. Chem.* 32 (2018) e3917.
- [44] K. Liu, L. Han, J. Zhuang, D.P. Yang, *Mater. Sci. Eng. C* 78 (2017) 429–434.
- [45] M. Guo, J. He, Y. Li, S. Ma, X. Sun, *J. Hazard. Mater.* 310 (5) (2016) 89–97.
- [46] H. Mao, C. Ji, M. Liu, Z. Cao, D. Sun, Z. Xing, X. Chen, Y. Zhang, X.M. Song, *Appl. Surf. Sci.* 434 (2018) 522–533.
- [47] J. Li, C. Liu, Y. Liu, *J. Mater. Chem.* 22 (2012) 8426–8430.
- [48] J. Jiang, G.H. Gunasekar, S. Park, S.H. Kim, S. Yoon, L. Piao, *Mater. Res. Bull.* 100 (2018) 184–190.
- [49] J. Singha, A. Mehtab, M. Rawata, S. Basub, *J. Environ. Chem. Eng.* 6 (2018) 1468–1474.
- [50] M. Mogudi, P. Ncube, R. Meijboer, *Appl. Catal. B: Environ.* 198 (2016) 74–82.
- [51] S. Giria, R. Dasa, C. Westhuyzenb, A. Maity, *Appl. Catal. B: Environ.* 209 (2017) 669–678.
- [52] N. Sahiner, O. Ozay, *Curr. Nanosci.* 8 (2012) 367–374.
- [53] B. Yoon, H. Hakkinen, U. Landman, *J. Phys. Chem. A* 107 (2003) 4066–4071.
- [54] H.H. Kim, S. Tsubota, M. Date, A. Ogata, S. Futamura, *Appl. Catal. A Gen.* 329 (2017) 93–98.
- [55] B. Zhu, J.-L. Liu, X.-S. Li, J.-B. Liu, X. Zhu, A.-M. Zhu, *Top. Catal.* 60 (2017) 914–924.
- [56] M. Ruan, P. Song, J. Liu, E. Li, W. Xu, *J. Phys. Chem. C* 121 (2017) 25882–25887.
- [57] J. Xia, G. He, L. Zhang, X. Sun, X. Wang, *Appl. Catal. B: Environ.* 180 (2016) 408–415.